Textures, fabrics and meltlayer stratigraphy in the Hans Tausen ice core, North Greenland – indications of late Holocene ice cap generation?

By Karen Nørgaard Madsen and Thorsteinn Thorsteinsson

Abstract

Madsen, K. N. and T. Thorsteinsson 2001. Textures, fabrics and meltlayer stratigraphy in the Hans Tausen ice core, North Greenland – indications of late Holocene ice cap generation? Copenhagen, Danish Polar Center. Meddelelser om Grønland Geoscience 39, pp. 97-114.

A thin section study of crystal structure has been carried out on a 345 m long ice core drilled to bedrock on Hans Tausen Iskappe, 1995. In addition a meltlayer stratigraphy was set up, showing how the fraction of meltlayer-ice in the core increases with depth. Main characteristics of crystal structure are increasing mean crystal size from top to bottom in the core and development of a weak single maximum c-axis fabric. The rate of ice crystal growth in the well dated upper half of the core is much lower than expected from studies of the normal grain growth regime in other polar ice cores. Probably the grain boundary movements are impeded by impurities, which are present in relatively high concentrations in the Hans Tausen ice. Asuming the applicability of the calculated growth rate throughout the core, a late Holocene origin of the oldest ice is suggested by the size of the crystals close to bedrock. Presented data furthermore implies that bottom ice temperatures were never near the melting point and it is concluded that there was no ice cap on the Hans Tausen plateau earlier in Holocene.

Keywords: Glaciologi; glacier ice crystals; grain growth: meltlayers; Holocene climate.

Karen Nørgaard Madsen, Department of Geophysics, Niels Bohr Institute for Astronomy, Physics and Geophysics, University of Copenhagen (Now: University of Bergen, Institute of Solid Earth Physics, Norway).

Thorsteinn Thorsteinsson, Alfred Wegener Institute, Geophysics division, Bremerhaven, Germany.

Introduction to Hans Tausen Iskappe

Hans Tausen Iskappe is located on a plateau in Pearyland, North Greenland. This irregularly shaped ice cap stretches out 75 km from north to south and 50 km from east to west, reaching elevations up to 1300 m a.s.l. (Thomsen *et al*. 1996). In the summer of 1995 an ice core was drilled on the southern dome of the ice cap. Drilling reached bedrock and the core retrieved is 345 m long. Temperatures in the Hans Tausen bore hole increase approximately linearly from

–21°C near the surface to –16°C at bedrock (Johnsen, S. J., personal communication 1997).

A visible feature of the core is the frequent occurrence of melt layers formed by refreezing of meltwater in the firn. In the present paper, ice formed in this way will be termed *meltlayer-ice*, while glacial ice formed by gradual compression of firn will be referred to as *firn-ice*. The abundance of meltlayer-ice in the core increases with depth (Fig. 1), attesting to warmer conditions at the surface earlier in the history of the ice cap.

Average $\delta^{18}O$ values of the ice are around $-27^0/_{00}$ in the upper $^3/_4$ of the core decreasing by $1^0/_{00}$ in the deepest part (Hammer *et al.* 2001). Considering the raised fraction of meltlayer-ice in the last part of the core the slight lowering of $\delta^{18}O$ values can hardly be interpreted as a transition to ice age conditions. Thus all ice within the core must have been deposited during the Holocene. For further dating of the ice core, time markers are provided by identified volcanic eruptions. Annual layer thicknesses in the core seem to be almost constant at 10-11 cm at least to the acidic peak at 131.5 m assigned to the 934 AD eruption of Eldgjá (Stampe 1997). Below this depth there are no clear guidelines for the time scale.

The purpose of this paper is to present and interpret data from thin section studies of the Hans Tausen Ice Core and discuss what can be learned about the ice cap from the crystal structure of the ice and the meltlayer stratigraphy. The analysis will be based on the hypothesis that the ice cap formed on the Hans Tausen plateau during the Holocene. Alternatively, the lack of depositions from the last ice age could be explained by melting and run-off from the bottom of the ice cap during the Holocene. This scenario is less appealing considering the present temperature at bedrock, but will however be evaluated in a later discussion of former temperatures in the ice.

Polycrystalline structure of glacial ice

The development of the polycrystalline structure has been investigated in several deep ice cores. Observations of crystal size variations with depth have revealed 3 recrystallization mechanisms, governing the movement or formation of crystal boundaries within the ice under various conditions (Herron & Langway 1982, Alley 1992).

In the top part of the ice cap, where strain and strain rates are small, mean crystal size is increasing with the age of the ice. Reduction in free surface energy by elimination of the smallest crystals provides the driving force for the process dominating, called *normal grain growth*. Following early results from metallurgy, it has been generally accepted to describe the growth of mean crystal size in firn and ice at low strain as function of time by

$$D^2 = D_0^2 + k\,t, \qquad (1)$$

where D_0 and D are mean crystal dimensions at time t_0 and $t > t_0$, respectively (Gow 1969, Alley 1986 et al., Alley 1992). However, it should be borne in mind that theoretical considerations have also led to other growth laws (Atkinson 1988, Alley et al. 1986), for instance with the exponent of 2 raised up to 3. It is very hard to argue for one growth law or the other by data, since the normal grain growth regime often corresponds to a quite limited time interval relative to the slow rate of growth. Put in another way the function relating mean crystal size to time can not be precisely determined because it is constrained by data in a window which is too narrow relative to the scale of its curvature, given the inevitable scatter of data. The local variability of crystal size is not just statistic fluctuations, but reflects the influence of other factors on crystal growth, one of which is impurities in the ice. By impeding crystal boundary migration, impurities lower the growth rate and could possibly change the functional

relationship too (Alley et al. 1986, Alley et al. 1995, Duval & Castelnau 1995).

Adopting equation (1), the growth rate k has been demonstrated to show an Arrhenius type temperature dependence expressed by

$$k = k_0 \, exp \left(\frac{-Q}{RT} \right), \qquad (2)$$

where Q is the activation energy for crystal growth, R the gas constant, T the temperature in Kelvins and k_0 a constant of proportionality (Gow 1969, Duval 1985, Paterson 1994, Li 1995). At temperatures above –10°C, experiments indicate that the grain growth rate increases much faster with temperature than predicted by (2) with k_0 and Q being the constants appropriate for lower temperatures (Li 1995).

Deeper in the ice cap, stored strain energy can provide new driving forces for recrystallization, changing the characteristics of the polycrystalline structure. Succeeding the initial growth a zone of stagnating mean crystal size is observed in several ice cores (Gow & Williamson 1976, Herron & Langway 1982, Alley 1992, Gow et al. 1997, Thorsteinsson et al. 1997). The occurrence of constant crystal size has been explained by the onset of *polygonization*, a process by which deformation induced dislocations arrange themselves into new crystal boundaries, leading to subdivision of crystals and thereby counteracting normal grain growth (Alley 1992, Alley *et al*. 1995).

Finally *dynamic recrystallization*, a process favoured by high strain/strain-rate and temperature is believed to overprint earlier crystal structure close to the bottom of a few drill sites in thick ice sheets. Due to the difference in stored strain energy, new and essentially strain free grains can nucleate in the matrix of highly strained older grains and expand rapidly to form large irregular crystals (Gow & Williamson 1976, Duval & Castelnau 1995, Gow *et al*. 1997).

Methods

The meltlayers are visible in the core as clear bands of essentially bubble free ice and were recorded in the field (H. B. Clausen, personal communication 1997). The total thickness of meltlayers was summed for each 55 cm of core (a bag length), and below the firn/ice transition this is immediately converted into a meltlayer percentage. In the top 60 m of the core the different density of meltlayer-ice and firn must be taken into account in order to obtain a meltlayer percentage, which is independent of the firn compression state. The correct weight percentage is obtained as $\rho_{ice}S_{ice}/(\rho_{ice}S_{ice} + \rho_{firn}S_{firn})$, where ρ and S denote density and core length of ice and firn. However, available density data dictated a more rough calculation of weight percentage replacing the denominator by the bag length times a density at the given depth estimated by the mean density profile of the core (Clausen, H. B., personal communication 1997). If the bag in question contains more (less) than average meltlayer-ice the denominator will be too small (large), thus the amplitude of meltlayer intensity variations is slightly exaggerated in the top.

For the study of ice crystal structure in the Hans Tausen ice core, a total of 34 vertical thin sections were cut parallel to the long axis of the core and evenly spaced from top to bottom. In addition 8 horizontal thin sections, normal to the long axis of the core and evenly spaced from 120 to 330 m were prepared for determining fabric. The coexistence of meltlayer-ice and firn-ice calls for separate analysis to investigate the influence of meltwater percolation on crystal growth. Thus the sampling was done with the aim of obtaining thin sections covering both meltlayer-ice and firn-ice when possible.

Mean crystal sizes were measured on vertical thin sections using the linear

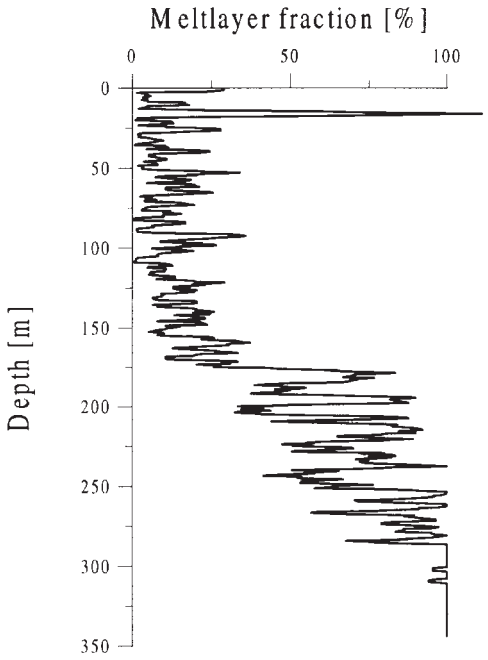

Fig. 1. Percentage by weight of meltlayer-ice in the Hans Tausen ice core, calculated in running mean of 2.20 m. A pronounced shift from high to low fractions of meltlayer-ice is encountered at 175 m depth. A short interval of very high melt is seen in the top at 15-17 m depth. The actual fraction of course does not exceed 100%, this is a consequence of the procedure used for air correction of the firn as explained in the section on methods. The vulcanic time horizon of Katmai 1910 eruption is identified closely below at 17.63 m depth.

intercept method by which the number N of crystal boundaries intersected by a test line of length L is counted. The linear intercept diameter, L/N, was used as a measure of mean crystal dimension. Using test lines parallel and normal to the long axis of the core, vertical and horizontal crystal dimensions D_v and D_h were obtained. Each measurement used several test lines across the thin section, with enough spacing to prevent the same crystal from being counted twice. In most cases this procedure allowed for at least 100 crystals to enter the measurement and the error is then less than 1 mm. The mean crystal diameter was defined as the geometric mean, $D=(D_h\ D_h\ D_v)^{1/3}$, implicitly assuming symmetry around the vertical. For convenience in relation to the growth law (1), D^2 will be referred to as the crystal size.

Crystallographic *c*-axis orientations were measured for the horizontal thin sections using standard operations on a semi automatic Rigsby Stage (Langway 1958, Lange 1988). In addition some extra measurements were carried out on vertical thin sections, noting for each *c*-axis measurement which crystal it belonged to by numbering the crystals on a photograph. This procedure provides the distribution of angles between neighbouring crystals which may reveal the possible recrystallization mechanisms responsible for the existing polycrystalline structure (Alley et al. 1995). If polygonization is happening to a considerable degree, an overweight of low angle boundaries is expected, relative to a sample with the same *c*-axis directions distributed randomly among the crystals. Dynamic recrystallization could also be detected by this method.

Observations

Meltlayer stratigraphy

The variation of meltlayer intensity with depth in the core is shown in Fig. 1. Note that the meltlayer curve is not a direct record of the annual meltwater formation, since the fraction of meltlayer-ice is modulated by changing accumulation. There is however a clear trend of increasing meltlayer abundance with depth, with a pronounced step to higher fractions encountered around 175 m depth. Below this point the oscillations of meltlayer intensity seem to proceed with higher amplitude until the core consists of 100% meltlayer-ice at 285 m depth. The remaining 60 m is superimposed ice interrupted only twice by a few cm of firn-ice.

A significant short term feature of the meltlayer curve is the shallow slim peak at 15-17 m depth. Based on volcanic signals (especially 1910 (Katmai) at 17.63 m and in addition 1873 at 23.05 m to estimate the rate of accumulation (Stampe 1997)) this meltlayer is dated to 1915-1930. The meltwater might have penetrated some meters down in the snow pack, which would make the melt event up to 10 years younger than the meltlayer, considering annual snow accumulation at the drill site.

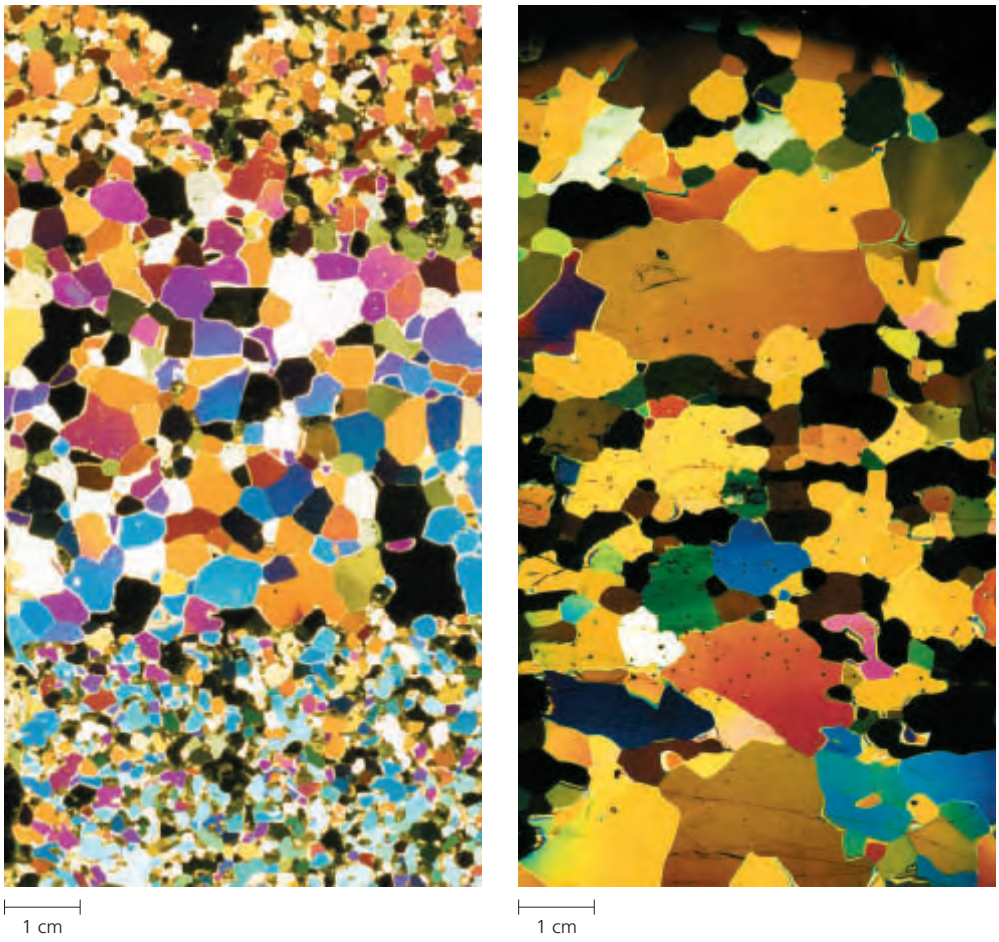

Fig. 2. Thin sections from increasing depths photographed between crossed polarizers. a: 26.40 m. Firn with a meltlayer clearly visible by its larger crystals. b: 209.65 m. Firn layer compressed to glacier ice surrounded by meltlayers with larger crystals. Air bubbles in the firn-ice are still seen. c: 285.50 m. Meltlayer-ice with a distinct difference in crystal size for top and bottom. c-axis measurements and chemistry data reveal that the appearance of smaller crystals is not associated with shear bands, but may be explained by contrasts in impurity concentrations. d: 329.95 m. Meltlayer-ice 15 m above bedrock with crystals being strikingly equant in size and shape.

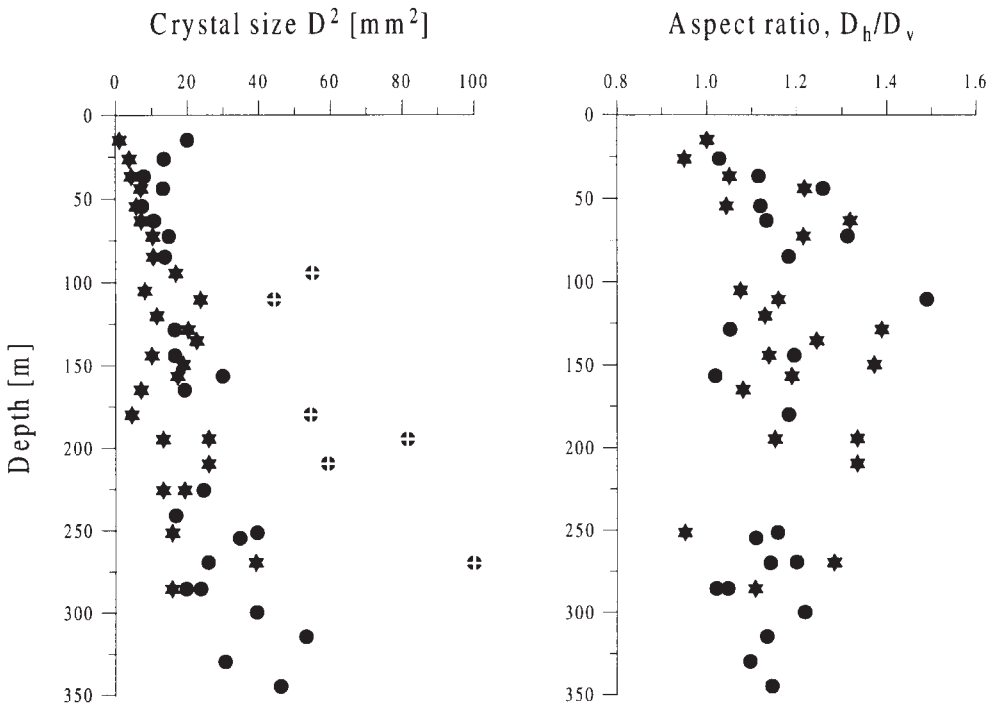

Fig. 3. Development of crystal size (as defined in the method section) and aspect ratios with depth in the core. Stars and dots denote data points obtained from firn-ice and meltlayer-ice respectively. Dots are marked with crosses for a group of outlier points which will be discussed later.

Crystal texture

In Fig. 2 photographs showing selected features of the crystal texture at different depths are reproduced. In the top 50 m, firn is not fully compressed to ice yet and displays small crystals, while the initial crystal size in the meltlayer-ice is considerably larger (Fig. 2a). Pronounced contrast in mean crystal size at the scale of thin sections is observed deeper in the core as well, coinciding with boundaries between meltlayer-ice and firn-ice (Fig. 2b) or totally within one kind of ice, most often meltlayer-ice (Fig. 2c). Strain shadows are observed at depths below 100 m, but become extinct 50 m above bedrock. In the last 50 m of the core, crystals are strikingly equant in size and shape (Fig. 2d), as if grown under very undisturbed conditions.

Fig. 3 shows to the left the crystal size profile along the core. There is a clear trend of mean crystal size increasing with depth and the growth is similar for firn-ice and meltlayer-ice although variations are clearly larger for the latter, featuring examples of outstanding large crystals around 100 and 200 m depth. Crystal elongation measured by the aspect ratio D_h/D_v increases over the top 50 m, but then stabilizes around 1.2, or perhaps decreases slightly towards the bottom.

c-axis distribution

In Fig. 4 the fabric diagrams obtained from *c*-axis measurements on the horizontal thin sections are displayed. All samples except the lowermost from 330 m depth have anisotropic *c*-axis distributions. The *c*-axes cluster in weak single maxima of similar strength throughout the core. Fabric development is summarized in the diagram to the left using the median polar angle θ_m as a measure of fabric strength. Additional data points in 210, 240 and 285 m depth are from measurements carried out on vertical thin sections to investigate if zones of smaller crystals could be shear bands. This was not the case. On

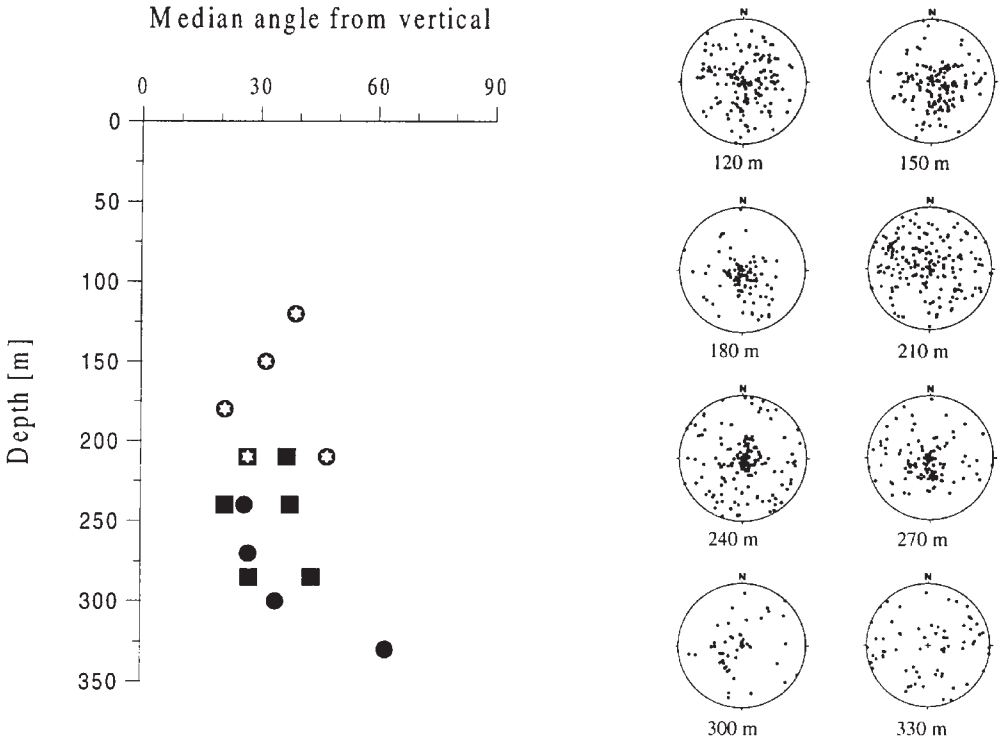

Fig. 4. Fabric diagrams obtained from the 8 horizontal thin sections and the change with depth of fabric strength given by the median angle θ_m, the top half angle in a cone around vertical containing half of the c-axes. A random distribution of c-axes corresponds to θ_m =60° while complete alignment has θ_m = 0°. Symbols with and without white stars denote data points from firn-ice and meltlayer-ice respectively. Extra data points (shown with squares) are obtained from additional measurements on vertical thin sections, rotated so that all data refer to the same coordinate system.

the contrary, the larger crystals in the thin sections from 240 and 285 m depth had the stronger fabric. They were associated with cleaner ice as well, which probably is the reason for the local size difference. In 210 m depth the crystal size contrasts were coincident with meltlayer boundaries and fabric was stronger in the firn-ice with the smaller crystals.

Fig. 5 represents the distribution of angles between *c*-axes of neighbouring crystals in the vertical samples from 210, 240 and 285 m depth. A strong fabric in itself dictates low angles between *c*-axes of individual crystals, whether they are neighbours or not. To investigate the possible influence of polygonization the distribution of angles between *c*-axes of neighbouring crystals must therefore be compared to the distribution of angles between *c*-axes of pairs of crystals picked randomly. This was done by repeating 10000 times a random selection of two crystals from the sample and calculation of the angle between their *c*-axes. The 10 intervals of angles in the figure are adjusted to make 10% of the 10000 angles fall in each interval. With no preferred angles between neighbouring crystals, their mutually angles should also be distributed equally among the 10 intervals and the relative frequencies would all be 1 except for the statistical variation. Dashed lines in the figures indicate the upper and lower fre-

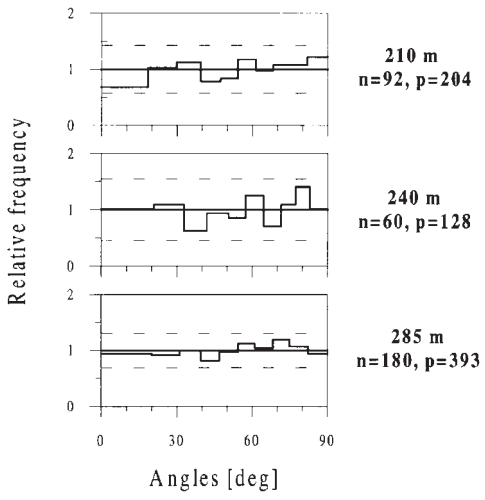

Fig. 5. Distribution of angles between neighbouring crystals in a sample normalized by the distribution of angles between crystals picked at random from the same sample (see text for further explanation). Measurements were carried out on samples from 210, 240 and 285 m depth. In each diagram the number of crystals (n) and neighbouring pairs (p) are noted. Notice that statistics are not equally good for the 3 datasets. Dashed lines indicate the level of significant deviation from a random distribution at 95% confidence level.

quency limits to be exceeded in an interval for the distribution to deviate from random with 95% confidence in a binomial test.

The measurements were carried out on samples from a depth interval where fabric has reached maximum strength according to Fig. 4 and the total deformation thus is expected to be at its highest. However no significant deviation from the random distribution is revealed by the data, especially not a preference for low angle boundaries, as would be expected if polygonization were altering the polycrystalline structure to a considerable degree.

Interpretation of the polycrystalline structure

Deformation and the recrystallization regime

Since the drill site is situated on top of a dome, compression is assumed to be the dominating stress system in accordance with observed fabric pattern. However, single maximum fabrics also form in simple shear. No strong *c*-axis alignment is revealed, which is to be expected for a newly formed ice cap with a limited strain history. An empirical relationship between vertical deformation and strength of the anisotropy developed is well established for relatively weak fabrics, and may be used to estimate the total compression of ice in the Hans Tausen ice core. Measured values of θ_m around 30° from 100 to 300 m depth correspond roughly to a total vertical deformation of 30-40% (Azuma & Higashi 1985, Castelnau et al. 1996). In the top 100 m, where unfortunately no fabric measurements have been carried out, strain is probably decreasing towards zero at the surface.

The random fabric measured in the sample 15 m above bedrock, the disappearance of strain shadows and the equant crystal texture in the last 50 m of the core are all signs of limited deformation of the ice close to the bottom. It may be that the drilled part of the ice cap is sitting in a bedrock depression, but low deformation close to bedrock can also be understood as a result of ice dynamics. If the ice cap has always been frozen to the bed, which seems reasonable considering the present temperature of –16° at bedrock, then vertical strain-rates are predicted to approach zero at the bottom of the ice cap. With a short history of deformation, total strain too is expected to be small close to the bedrock. Thus undisturbed crystal growth conditions for ice in the lowermost part of the core may be accounted for by a simple ice flow model.

As has been observed in other ice cores (Hooke & Hudleston 1981, Lipenkov et al. 1989, Thorsteinsson 1996), the ice crystals are generally less elongated than would be expected considering the inferred total strain. If the crystal structure were stationary except for deformation (that is no grain growth, polygonization, etc) and flattening of each crystal simply followed bulk deformation, the grain boundaries beeing passive strain markers, then the aspect ratio of crystal shape would increase with total strain by uniaxial compression as indicated by the solid line in Fig. 6.

By normal grain growth the material positions of grain boundaries are moving and isotropic growth could be argued to slow down the flattening of crystals, since an elongate crystal becomes rounder by growing the same amount in all directions. The dotted lines in Fig. 6 indicate the development of aspect ratio with total strain for strain rates ranging from 10^{-2} to 10^{-5}. The examples shown are all starting from a spherical crystal of diameter 3 mm and assuming a mean area (in vertical thin section) growth rate of 10^{-2} mm^2/year, which is appropriate for Hans Tausen conditions as will be seen later. What matters for the calculation however is

only the mutual proportions between the rate of crystal growth and the rate of compression. Still using the Hans Tausen ice core as an example it appears that even with the modification introduced by growth of the crystals, the observed aspect ratio 1.2 suggests that total strain should be less than 15%, which is much less than indicated by fabric strength. For a total strain of 30-40% in accordance with general fabric strength measured in the core, the aspect ratio in this model would exceed 1.5. This is more than observed anywhere in the core. Clearly the model is not in agreement with data.

Polygonization operating to some degree along with the normal grain growth could be the mechanism keeping the aspect ratio low by subdividing elongated crystals. In that case the notion of 'onset of polygonization' would be misleading. Rather polygonisation would be an active process well up in zone of crystal growth, gradually gaining influence with increasing depth until a balance with normal grain growth is obtained resulting in a stagnation of crystal size. Another possibility is that some feature of normal grain growth itself counteracts the development of strongly elongated crystals. The possible influence of polygonisation or other process keeping the aspect ratio low in the so called normal grain growth regime is a general problem, which needs further investigation in order to reveal to what extent the crystal growth rate is affected.

The steady growth of mean crystal size with depth in combination with weak single maximum fabrics, are observations that usually are inferred to indicate that normal grain growth is the dominant process controlling the development of the polycrystalline structure. However an effect of polygonization can not be excluded even though a stagnation of crystal sizes is not seen. Depths of 200-300 m are in the zone expected to be most susceptible for polygonization due to a combination of high strain-rate and high strain, but the investigation of the angles between c-axes of neighbouring crystals in this depth interval failed to reveal any influence of polygonization. On the other hand strain shadows observed from 100 to 300 m could be a sign of beginning polygonization. If active, pologonization may or may not change the functional relationship (1). Since too little is known about the influence of polygonization in the zone where crystals are still growing, crystal data will be analyzed assuming the applicability of the normal grain growth law (1). Subsequently some polygonization scenarios and their impact on the conclusions of the analysis will be discussed.

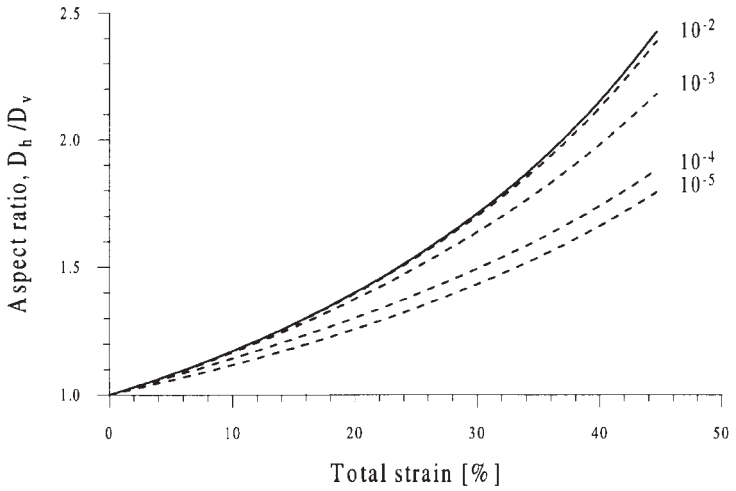

Fig. 6. Aspect ratio of a volume deforming in uniaxial compression as function of total strain ($(a-a_0)/a_0$, a_0 and a being thichness before and after compression). The solid line apply to the bulk of the ice or a crystal following bulk deformation. Dotted lines indicate the development of shape, when isotropic growth of the volume happens simultaneous with the compression. The growth rate and the initial crystal size are chosen to match Hans Tausen conditions ($k=10^{-2}$ mm^2/year and $D_0=3$ mm^2 and strain rates are 10^{-2}, 10^{-3}, 10^{-4} and 10^{-5} year^{-1} respectively).

Factors affecting mean crystal size locally

In the top 50 m of the Hans Tausen ice core, mean crystal size is significantly larger in meltlayers than in the surrounding firn. It seems impossible that temperature enhancement of normal grain growth can account for the initial size difference, even if latent heat released by refreezing of meltwater would raise the temperature close to the

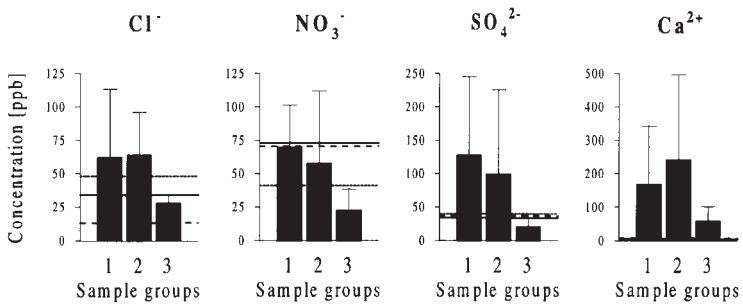

Fig. 7. Mean values and standard deviations for concentrations (ppb) of Cl^-, NO_3^-, SO_4^{2-} and Ca^{2+} in samples 1) firn-ice, 2) meltlayer-ice excluding the outliers of Fig. 3 and 3) meltlayer-ice, outliers. Dashed, dotted and solid lines indicate background levels of the same ions in Holocene ice from Summit (Whitlow et al. 1992), Byrd Station and Camp Century (Paterson 1991) respectively.

melting point. Growth rates as high as 30 mm^2 per year at –0.2°C have been reported (Li 1995), but still months are needed for the crystals in meltlayers to gain the lead of 10-20 mm^2 in crystal size. It is hard to believe that the heat will stay localized in the meltlayer for that long, which would be necessary to explain why the adjacent firn does not grow large crystals. More likely the large crystals are created in the very process of refreezing meltwater.

Deeper in the core the crystal size contrast between firn-ice and meltlayer-ice is often less pronounced or even absent. By equation (1), a blurring of initial crystal size differences with depth is to be expected, since with increasing age of the ice the constant term D_0^2 becomes negligible compared to the growth term $k\,t$. Size contrasts encountered in older ice must owe to local variations in the growth rate. Any difference in growth rate is magnified by the age of the ice, leading to the increased scattering of crystal sizes with depth, revealed by Fig. 3. Local variations of the growth rate are possibly due to different impurity concentrations. Redistribution of impurities is likely to occur with the percolation of meltwater, which might explain why the larger variations of crystal size are associated with the meltlayer-ice.

A comparison of impurity concentrations has been made between samples from the group of outlier points in Fig. 3 and samples from the remaining part of the meltlayer-ice and from firn-ice. Impurities investigated were Cl^-, NO_3^-, SO_4^{2-}, Ca^{2+}, Na^+, K^+, Mg^{2+}, NH_4^+ and micro particles (0.4-2.0 μm). The content of insoluble dust shows no difference among the groups, while all ions excluding ammonia are rarefied in the outlier group, as exemplified by Fig. 7 showing plots of mean concentrations and standard deviations for Cl^-, NO_3^- and SO_4^{2-}. It should be noted that the considerations presented here rest on a meager data material due to the limited amount of data from the group of outliers and furthermore that the redistribution of impurities taking place by meltwater percolation could lead to very localized accumulations of impurities making bulk measurements misleading. However the measurements do support the idea that the outliers are associated with spots of unusually clean ice.

Analysis of the crystal growth

Crystal data were analyzed applying the normal grain growth law (1). To determine the growth rate of mean crystal size, a dating of the ice is required. Furthermore, the influence of temperatures changing with depth and time needs to be evaluated.

Tentative dating of the ice

The eruptions of Laki (1783 AD) encountered at 35.1 m depth and Eldgjá (934 AD) at 131.4 m depth provide two major fix points for the time scale (Stampe 1997, Clausen et al. 2001). Following the hypothesis of a newly formed ice cap, a tentative dating was obtained by modelling the generation of an ice cap which has a thickness at the ice divide given by the length of the Hans Tausen ice core, the time horizons mentioned above placed at right depths and a profile of total strain in accordance with observed fabric strength in the core (Madsen 1997). The growth of a very simplified Hans Tausen ice cap was modelled using a vertically integrated flow model

(Oerlemans 1981). Subsequently the Dansgaard-Johnsen model was invoked to follow the downward movement of individual time horizons within the ice column at the drill site (see e.g. Paterson 1994). Adjusting the dependence of accumulation on elevation, a variety of possible time scales for the older part of the core can be extracted from the modelling. Two examples shown in Fig. 8 will be considered in this paper. The first one ascribe an age of 3500 years to the ice close to bedrock. It turns out from the modelling (or from a rough calculation) that this timescale represents a lower age limit. Generating the present ice thickness considerably faster require early accumulation rates far exceeding present precipitation.

On the other hand stretching the time scale to older ages is possible. The example shown spans 5500 years, and even longer time scales can be obtained.

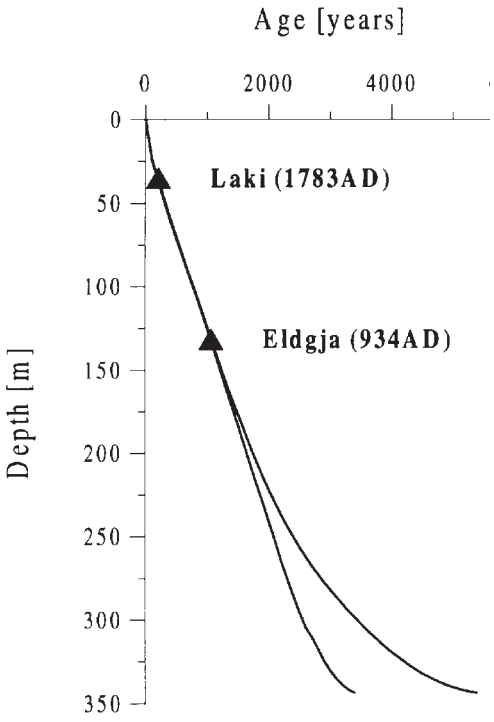

Fig. 8. Two possible time scales of total length 3500 and 5500 years for the Hans Tausen ice core, obtained by modelling the generation of the ice cap. The time horizons provided by eruptions of Laki (1783 AD) and Eldgjá (934 AD) are marked with vulcanic cones.

Temperature correction to crystal growth

Due to the strong temperature dependence of crystal growth given by equation (2), data should be corrected for the different temperature histories experienced by crystals at different depths. Considering only the increasing elevation of the ice surface and using a lapse rate of 0.75°C/100 m, the early ice cap had a temperature around –18.5°C, increasing at the bottom and decreasing at the top as the ice cap grew. The movements of the ice crystals downwards in the ice cap were extracted from the modelling. Temperature profiles back in time were taken to be steady state profiles (see e.g. Paterson 1994), with parameters adjusted to fit the present temperature curve and former surface temperatures based on the modelled surface elevation. Latent heat released by refreezing of melt water has not been taken into account explicitly, and neither has any climatic change been assumed. Invoking the temperature correction, equation (1) is changed to

$$D^2 = D_0^2 + k_0 \sum exp\left(\frac{-Q}{RT}\right) \Delta t, \qquad (3)$$

summing over the time span in which the crystals have existed, or

$$D^2 = D_0^2 + k_0 \bar{A}_t \, t, \qquad (4)$$

where $\bar{A}$ is the time averaged Arrhenius factor for the crystals of age t. The activation energy, Q, was found by regression analysis on data from five other polar ice cores in which crystal growth rates have previously been determined (Fig. 10. The growth rate for Hans Tausen ice core, to be derived in the following, is also displayed but of course not included in this evaluation of Q). According to equation (2) data should define a straight line of slope $-Q/R$ in a plot of k on logarithmic scale versus $1/T$. The fit to data in Fig. 10 is very satisfactory and results in the value Q=58 kJ/mol. Previous analyses using other dataset have suggested lower values of Q (Gow 1969, Duval 1985, Paterson

1994). However this analysis uses data from ice only rather than data from firn or mixtures of data from ice and firn and cores covering both ice and firn. A satisfactory demonstration that ice crystal growth in firn and ice follow the same growth law is not known to the authors.

Furthermore it has been avoided to plot data multiplied by different correction factors used by some authors and an attempt has been made to convert the linear intercept measurements from GRIP to represent results obtained by mean area measurements, which have been used to obtain the other data. For these reasons Q=58 kJ/mol is considered the best value available for this purpose. Using it the present temperature span in the Hans Tausen bore hole make crystal growth 1.7 times faster close to bedrock than in the top of the ice core. By the temperature correction derived above, time averaged crystal growth rates increase from top to bottom by a factor 1.4 using the shorter time scale and slightly less using the longer.

The rate of crystal growth in the upper 200 m

Growth rates were calculated by fitting equation (4) to data. The analysis was restricted to the upper 200 m of the ice core, for which the time scale is well established and the temperature correction small in any circumstance. Data points from firn not yet transformed to ice have been excluded. For firn-ice the growth rate $7.9 \cdot 10^{-3}$ mm^2/year at –21°C was derived from the fit shown to the left in Fig. 9. As already discussed data from meltlayer-ice are more scattered. However from Fig. 3 it is evident that, excluding the outliers, crystal sizes in meltlayer-ice follow the same trend of growth as crystal sizes in firn-ice.

Fig. 9 shows to the right a fit to data from meltlayer-ice in the upper 200 m using the growth rate obtained for firn-ice but taking into account the larger initial size by raising D_0. The fit is good for most of the crystals, while the smaller group of outliers treated separately indicate a much faster growth – perhaps 3 times faster. It should be noted that the

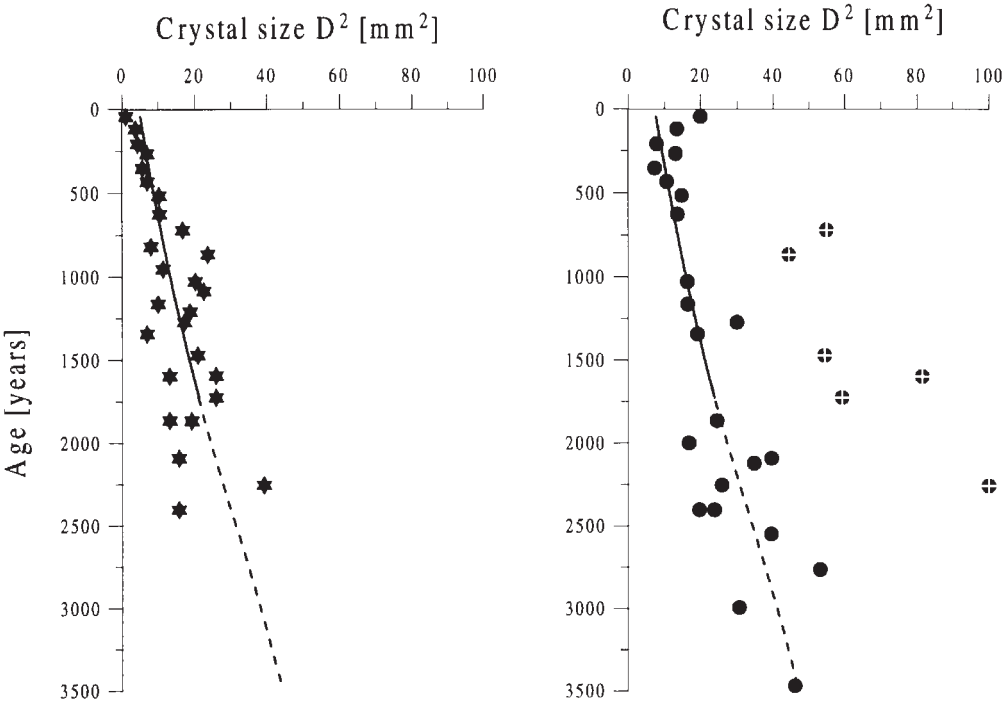

Fig. 9. Crystal sizes (mm^2) versus ascribed age of the ice (years B.P.). The solid line show the best fit of the growth law (3) to data. The timescale used in this figure is the younger of the modelled time scales shown in Fig. 8, but the choice has no importance for the fit which is restricted to the top 200 m, where the time scales are in good agreement. Left: Data from firn-ice. The fit was made excluding the first three data points from firn and data points obtained from ice below 200 m. Right: Data points from meltlayer-ice. The best fit was determined with k_0 fixed at the value found for firn-ice. The fit was made using only data points from the top 200 m and excluding the outliers (marked with white crosses). The dashed line is the extrapolation of the growth law beyond 200 m depth where time control is lost, i.e. it represents the expected crystal size as a function of time. Note that the prediction includes the effect of calculated temperature changes. With the depicted choice of timescale for the older ice, data are well described by this model. Associating the lower datapoints with higher ages (moving them downwards in the figure) would introduce a discrepancy with the model (crystal sizes would be smaller than predicted).

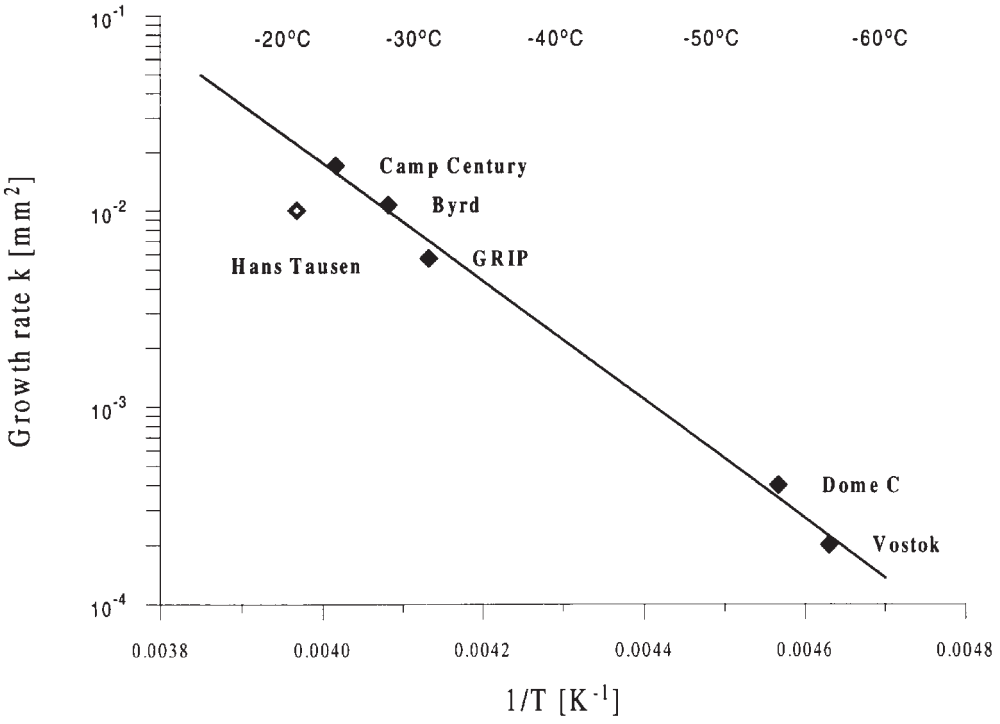

Fig. 10. Crystal growth rates in polar ice. Data points from Vostok (Lipenkov et al. 1989, crystal growth rate estimated by the authors using the published crystal size profile.), Dome C (Duval & Lorius 1980), Byrd (Gow & Williamson 1976), GRIP (Thorsteinsson et al. 1997), Camp Century (Herron & Langway 1982), and the regression line for these data. Also shown is the new data point from the Hans Tausen ice core. Data are given by mean area measurements (number of crystals per area). A correction factor of 1.29 obtained from studies of thin sections from the Hans Tausen ice core, has been applied to convert the linear intercept growth rates from Hans Tausen and GRIP to represent mean area results.

measurements of the largest crystals are inaccurate, since the requirement that crystal size should be much smaller than thin section dimensions is not met.

As can be seen from Fig. 10, the new data point from Hans Tausen ice core deviates appreciably from the regression line of previous data, the growth rate having only half the value expected from the regression line at –21°C. The most obvious explanation for this deviation is offered by the impurities in the ice impeding grain boundary motion. The general impurity level of the Hans Tausen ice core is relatively high compared to the other cores represented in Fig. 10, which are all retrieved from less exposed inland drill sites. The fact that the outlier data points of extremely large crystals in the meltlayer-ice are associated with spots of unusually clean ice lends further support to this explanation. Alternatively polygonization operating to some degree in the upper half of the core, could result in a lowered growth rate. In this case however the question is left why polygonization should not keep crystals small in the cleaner ice as well as in the rest of the core? In fact strain shadows are not absent in the very large crystals.

In case of impurity hindered grain growth, the impurity concentrations in the Hans Tausen samples could be compared with background impurity levels of the other cores from Fig. 10 in order to investigate which impurities have the main impeding effect on crystal growth. In Fig. 7 general concentrations of Ca^{2+}, Cl^-, NO_3^- and SO_4^{2-} in Holocene ice from GRIP, Camp Century and Byrd Station have been marked in the diagrams showing the concentrations in Hans Tausen ice core. In comparison to these two drill sites, the concentration of NO_3^- is not unusually high in Hans Tausen ice. Mean concentrations of Ca^{2+} are an order of magnitude higher in Hans Tausen ice than in GRIP ice, but since this is also the case for the group of outlier samples with high growth rates, Ca^{2+} is probably not the main cause of

impeded grain growth. SO_4^{2-} and to a less extent Cl^- ions are present in elevated concentration except in the outlier samples and thus could be the cause of the lowered growth rate. It may be noted that (Paterson 1991) concluded that elevated concentrations of Cl^- and possibly SO_4^{2-} in ice-age ice relative to Holocene ice kept crystals small and thereby caused the different rheology of the two types of ice.

Implications of data concerning Hans Tausen Iskappe

Age of the ice cap

Age estimates of Hans Tausen Iskappe may be evaluated based on crystal sizes in the ice close to bedrock, using the growth rate $k=7.9 \cdot 10^{-3}$ mm^2/year. From the two examples of time scales shown in Fig. 8, the one dating the oldest ice to 3500 years was selected for Fig. 9 because it happened to fit the data points in the older ice reasonably well. Fig. 11 displays what happens when the time scale is stretched from 3500 to 5500 years. The difference between measured and calculated crystal size is shown as a function of age of the ice for each of the two time scales. The longer time scale tends to predict larger crystals than found, while the shorter time scale leads to an even distribution of crystals being larger and smaller than calculated, and so appears to be a better dating.

The above estimate of the age of Hans Tausen Iskappe rests on the assumption that the growth rate determined in the previous section is applicable throughout the core meaning that temperature and age are the only depth dependent variables controlling crystal size. This involves that the impurity level and the degree of polygonization is approximately constant throughout the core. The concentrations of soluble impurities in the lower samples are comparable to the level in the upper part (excluding the very clean outlier samples), which justifies the growth rate used. As previously discussed, reduction of mean crystal sizes due to polygonization can not be ruled out. The importance of this effect for the age evaluation depends on the distribution of significant polygonization in the core. The age estimate is not affected if polygonization is equally active everywhere so that the functional relationship (2) is preserved and the only influence of polygonization is a smaller (but still constant) k. Data from the top of the core (where strain has not reached its maximum) are used for calculating the growth rate and crystal sizes close to the bottom (where strain apparently is low) are crucial for estimating the time of ice cap initiation. The age evaluation does not depend heavily on crystal sizes in the lower-mid sector where polygonization is likely to be strongest. If significantly more polygonization happens close to bedrock than in the upper part of the core, then the calculated growth rate will be too high for application in the oldest ice and thus the age estimate will be too low. The opposite case of less polygonization at the bottom than in the upper part of the core would lead to overestimating the age. However realistic time of formation can not be much lower than 3500 years.

Paleo ice temperatures

The temperature correction applied in the analysis presented above did not take into account latent heat when estimating former surface temperatures. Released latent heat from refreezing of meltwater may lead to a warming of average 0.266°C per cm meltlayer formed (Reeh 1990). Until 170 m depth the meltlayer fraction is small and similar to present conditions (Fig. 1), and additional warming may be neglected without major errors. Below 170 m the

amount of meltlayer-ice increases to 50-100% and latent heat may have raised the temperature of the ice significantly. Including latent heat in the calculation would add only minor corrections to the calculated growth rate based on the upper half of the core, while temperature enhancement of crystal growth in the older part of the ice has been larger than assumed. Thus the temperature correction applied in the above analysis can be considered a minimum correction.

Explaining observed crystal size by equation (4), a higher temperature correction $\bar{A}_t$ for ice at the bottom implies that the age of the ice is lower by the same factor. As paleo ice temperatures and age of the ice constrain each other in this way, and since the ice cap can not be much younger than the 3-4000 years suggested using the 'minimum' temperature correction, it follows that former ice temperatures can not have been much higher than assumed in the above. Particularly this implies that the total dominance of meltlayer-ice in the bottom of the core should not be interpreted as the remains of a former temperate glacier. Independently of the age estimate it can be argued that according to equation (2) and the results of (Li 1995) the crystal growth rate is one to several orders of magnitude larger at the melting point of the ice than at present temperatures in the bore hole, which means that after a few centuries (or even years) spent close to the melting point, the crystals would have grown larger than observed anywhere in the core. Finally it may be added that removal of older ice by bottom melting involves a substantial temperature drop at bedrock from 0°C when melting ceased to –16°C at present. Allowing the oldest ice in the core some thousands years to sink from the surface to the bottom before melting stops leaves quite a short period for this temperature drop.

In conclusion Hans Tausen Iskappe could have been warmed a few degrees by the latent heat of meltwater in its early days, strengthening the argument for a late formation of the ice cap, but a warming extensive enough to raise the temperature close to 0°C within the ice is not compatible with observed crystal sizes. Thus the lack of depositions from the ice age is hardly due to melting and run-off from the bottom of the ice cap.

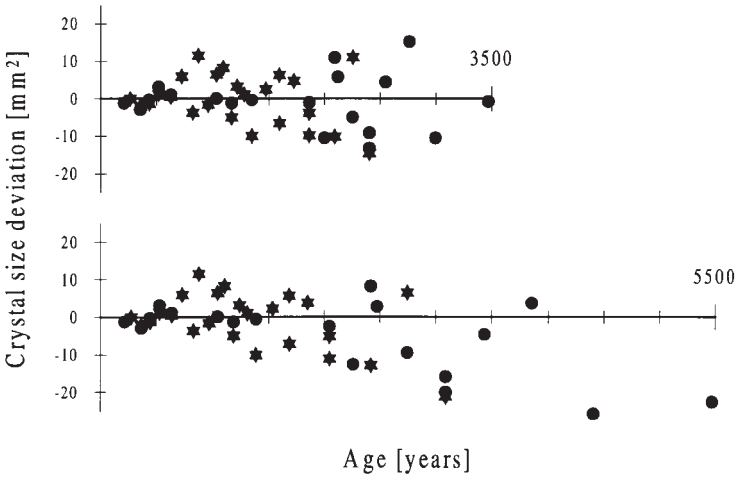

Fig. 11. Deviation of measured crystal size from the size calculated using each of the two timescales of Fig. 8. Stars refer to data from firn-ice and circles to meltlayer-ice. The deviations tend to grow with time, as expected from equation (1), since any initial difference in growth rate is magnified by the age of the ice. Crystals smaller and larger than calculated are evenly distributed in the upper plot, applying the time scale of 3500 years for the data analysis, while negative deviations dominate in the lower plot using the longer time scale of 5500 years.

Paleo accumulation and melt rates

Paleo accumulation rates control the lower limit of the age of Hans Tausen Iskappe, by the time needed to generate the appropriate amount of ice. To account for the deformation indicated by fabric development, mean accumulation is required to be higher than the present 10.8 cm ice equivalent per year if the ice cap is as young as indicated by the crystal data. Evidence that accumulation rates were indeed higher earlier in the history of the ice cap, comes from the constant layer thickness in the core to at least 130 m and probably as deep as 225 m (Clausen et al. 2001). In combination with a vertical compression as revealed by fabric data, this indicate that the accumulation could have been up to twice the amount precipitated at present. A more thorough investigation of fabric strength including the upper 100

m could provide more precise estimates of paleo accumulation.

With the graduation of accumulation mentioned above the meltlayer stratigraphy of Fig. 1 indicates that meltwater formation has decreased over the last thousand years probably around 50%. Provided that accumulation was never appreciably lower than the present, melting activity was even higher further back in time. This pattern conform to the history of a growing ice cap, subject to extensive summer melting until the surface is elevated well above the equilibrium line.

The meltlayer profile holds a climate record of (maximum) summer temperatures (Koerner 1977, Koerner & Fisher 1990). To draw conclusions concerning long term climate from the meltlayer record the effect of changing surface elevation due to the growth of the ice cap must be subtracted. Some studies have been made on the Queen Elizabeth ice caps, Canada (Koerner 1979), which show that the meltwater formation decreases exponentially with ice surface elevation. A quantitative applicability of these results to Hans Tausen Iskappe is questionable, but it seems likely that an exponential or other non-linear relationship between meltwater formation and elevation of the ice surface accounts for some of the highly elevated fraction of meltlayer-ice in the lower half of the core. However the change from approximately 10% to more than 50% meltlayer-ice encountered at 170 m depth in the core still seem so rapid that its explanation must involve some abrupt change, for instance of summer temperatures or accumulation. The higher amplitude of the oscillations in meltlayer intensities coincident with the shift to high meltlayer fractions are also worth noting. Is it attesting to an increased sensitivity of the meltlayer proxy below some critical point or is it the actual record of higher climatic variability in the past? To be able to infer paleo climate and/or the growth history of the ice cap from the meltlayer data, investigation of present meltlayer formation as a function of elevation on Hans Tausen Iskappe would be most useful.

Summary and conclusions

The increase of mean crystal size with depth throughout the Hans Tausen ice core suggests that the development of the polycrystalline structure of the ice is dominated by normal grain growth. Although strain shadows are observed in most of the core, the effect of polygonization seems limited but can not be excluded. The deepest 50 m of the core appear almost unaffected by strain. With the exception of a random *c*-axis fabric measured in ice 15 m above bedrock, fabrics observed below 100 m depth are weak single maximum fabrics which could have been created by vertical compression of the order of 30%. In combination with the knowledge of the thickness of annual layers in the core at least to the horizon of Eldgjá 934 AD eruption, this implies that accumulation has formerly been appreciably higher than present.

The growth rate of mean crystal size was calculated using linear intercept measurements in the well dated upper half of the core. The obtained value of $7.9 \cdot 10^{-3}$ mm^2/year at –21°C is only half the rate expected from previous studies of crystal growth in other polar ice cores. Soluble impurities especially SO_4^{2-} and Cl^- is found in relatively high concentrations in the Hans Tausen ice and may cause the low growth rate by impeding grain boundary motion. Explaning the slow crystal growth by impurities rather than polygonization partially counteracting normal grain growth is supported by the existence of outstanding large crystals associated with spots of unusually clean ice.

Provided that the effect of polygonization is negligible or approximately con-

stant throughout the core, the age of the oldest ice can be evaluated based on mean crystal sizes measured in the lower part of the core. It appears that the crystal size profile is in good agreement with a time scale of length 3500 years, but not with one reaching back 5500 years. Assuming the ice to have formerly been at the melting point at bedrock leads into contradiction with observed crystal sizes in the older part of the core, so the lack of ice age ice in the core is hardly explained by melting and run-off from the bottom of the ice cap. Thus the conclusion of this study is that Hans Tausen Iskappe was absent for a period in Holocene and (re)formed at a time conforming well to the 'Neoglacial' cooling 3500-4500 BP (Crowley & North 1991), which could have caused the initiation of the present ice cap. At the Hans Tausen plateau this climatic cooling could have been reinforced by the isostatic uplift of the area, that has been going on since the retreat of the inland ice at the termination of the last ice age (Funder & Hansen 1996). To learn more about late Holocene climate from the Hans Tausen ice core the meltlayer stratigraphy should be studied further.

Acknowledgements

We thank Marie-Louise Siggaard Andersen for measurements of impurity concentrations and Dorthe Dahl-Jensen and Michael Stampe Skousen for computational assistance and valuable discussions. Contribution no. 1535 of the Alfred Wegener Institute.

References

Alley, R. B. 1992. Flow-law hypotheses for ice-sheet modelling. *Journal of Glaciology* 38(129): 245-256.

Alley, R. B., A. J. Gow and D. A. Meese 1995. Mapping c-axis fabrics to study physical processes in ice. *Journal of Glaciology* 41(137): 197-203.

Alley, R. B., J. H. Perepezko and C. Bentley 1986. Grain growth in polar ice: I. Theory, II. Application. *Journal of Glaciology* 32(112): 415-433.

Atkinson, H. V. 1988. Theories of normal grain growth in pure single phase systems. *Acta Metallurgica* 36(3): 469-491.

Azuma, N. and A. Higashi 1985. Formation processes of ice fabric pattern in ice sheets. *Annals of Glaciology* 6: 130-134.

Castelnau, O., T. Thorsteinsson, J. Kipfstuhl and P. Duval 1996. Modelling fabric development along the GRIP ice core, central Greenland. *Annals of Glaciology* 23: 194:201.

Clausen, H. B., M. Stampe, C. U. Hammer, C. S. Hvidberg, D. Dahl-Jensen and J. P. Steffensen 2001. Glacial chemical studies on ice cores from Hans Tausen Iskappe. Meddelelser om Grønland Geoscience, this volume, pp 123-149.

Crowley, T. and G. R. North 1991. *Paleoclimatology* Oxford University Press. pp. 67-68, 92-94.

Duval, P. and O. Castelnau 1995. Dynamic recrystallization of ice in polar ice sheets. *Journal de Physique IV* 5(C3): 197-205.

Duval, P. 1985. Grain growth and mechanical behaviour of polar ice. *Annals of Glaciology* 6: 79-82.

Duval, P and C. Lorius 1980. Crystal size and climatic record down to the last ice age from antarctic ice. *Earth and Planetary Science Letters* 48: 59-64.

Funder, S and L. Hansen 1996. The Greenland ice sheet – a model for its culmination and decay during and after the last glacial maximum. *Bulletin of the Geological Society of Denmark* 42: 137-152.

Gow, A. J. 1969. On the rates of growth of grains and crystals in south polar firn. *Journal of Glaciology* 8(53): 241-252.

Gow, A. J., D. A. Meese, R. B. Alley, J. J. Fitzpatrick, S. Anandakrishnan, G. A. Woods and B. C. Elder 1997. Physical and structural proporties of GISP2 ice core: A review. *Journal of Geophysical Research* 102(C12): 26, 559-26, 575.

Hammer, C. U., S. J. Johnsen, H. B. Clausen, D. Dahl-Jensen, N. Gundestrup and J. P. Steffensen 2001. The paleoclimatic record from a 345 m long ice core from the Hans Tausen Ice Cap. Meddelelser om Grønland Geoscience, this volume, pp. 87-95.

Herron, S. L. and C. C. Langway 1982. A

comparison of ice fabrics and textures at Camp Century, Greenland and Byrd Station, Antarctica. *Annals of Glaciology* 3: 118-124.

Hooke, R. L. and J. P. Hudleston 1981. Ice fabric from a borehole at the top of the south dome, Barnes Ice Cap, Baffin Island. *Geological Society of American Bulletin Part I*, 92: 274-281.

Koerner, R. M. 1977. Devon Ice Cap: Core stratigraphy and paleoclimate. *Science* 196: 15-18.

Koerner, R. M. 1979. Accumulation, ablation and oxygen isotope variations on the Queen Elizabeth Islands ice caps, Canada. *Journal of Glaciology* 22: 25-41.

Koerner, R. M. and D. A. Fisher 1990. A record of Holocene summer climate from a Canadian high-arctic ice core. *Nature* 266: 508-511.

Lange, M. 1988. A computer-controlled system for ice-fabric analysis on a Rigsby Stage. *Annals of Glaciology* 10 : 92-94.

Langway, C. C. 1958. *Ice fabrics and the universal stage*. Thecnical Report 62, U. S. Army snow and permafrost establishment.

Li, J. 1995. *Interrelation between flow proporties and crystal structure of snow and ice*. PhD thesis, The University of Melbourne.

Lipenkov, V. Y., N. I. Barkov, P. Duval and P. Pimienta 1989. Crystalline texture of the 2083 m ice core at Vostok Station. *Journal of Glaciology* 35(121): 392-398.

Madsen, K. N. 1997. *Hans Tausen iskernen – studier af krystalstruktur, datering og smeltelagsstratigrafi*. Master of Scince thesis, University of Copenhagen.

Oerlemans, J. 1981. Some basic experiments with a vertically integrated ice sheet model. *Tellus* 33: 1-11.

Paterson, W. S. B. 1991. Why ice-age ice is sometimes 'soft'. *Cold regions Science and Technology* 20: 75-98.

Paterson, W. S. B. 1994. *The physics of glaciers*. Pergamon, 3. edition.

Reeh, N. 1991. Parametrization of melt rate and surface temperature on the Greenland ice sheet. *Polarforschung* 59(3): 113-128.

Stampe, M. 1997. Vulkanske vidnesbyrd i en iskerne fra Hans Tausen. Master of Science thesis, University of Copenhagen.

Thomsen, H. H., N. Reeh and O. B. Olesen 1996. *Glacier and climate research on Hans Tausen Iskappe, North Greenland – 1995 glacier basin activities and preliminary results*. Bulletin Grønlands geologiske Undersøgelse.

Thorsteinsson, T. 1996. *Textures and fabrics in the GRIP ice core, in relation to climate history and ice deformation*. PhD thesis, Alfred-Wegener-Institut für Polar und Meeresforschung.

Thorsteinsson, T., J. Kipfstuhl and H. Miller 1997. Textures and fabrics in the GRIP ice core. *Journal of Geophysical Research* 102(C12): 26,583-26,599.

Whitlow, S. P., A. Mayewski and J. E. Dibb 1992. A comparison of major chemical species seasonal concentration and accumulation at the South Pole and Summit, Greenland. *Atmospheric Environment* 26A: 2045-2054.